Available online at website: https://journal.bcrec.id/index.php/bcrec

Bulletin of Chemical Reaction Engineering & Catalysis, 21 (1) 2026, 168-179

Original Research Article

# Catalytic Performance of Environmentally Friendly Calcium Sulfate Hemihydrate-supported Metals (Ti, Fe, Cu or Ag) for Oxidation of Styrene to Benzaldehyde

**Agung Rahmadani[1], Mukhamad Nurhadi[1,*], Teguh Wirawan[2], Wirhanuddin[1], Nabila Nur Agusti[3], Sin Yuan Lai[4], Hadi Nur[5,6]**

*[1]Department of Chemical Education, Universitas Mulawarman, Kampus Gunung Kelua, Samarinda, 75119, East Kalimantan, Indonesia.*
*[2]Department of Chemistry, Universitas Mulawarman, Kampus Gunung Kelua, Samarinda, 75119, East Kalimantan, Indonesia.*
*[3]Department of Chemical Engineering, Universitas Mulawarman, Kampus Gunung Kelua, Samarinda, 75119, East Kalimantan, Indonesia.*
*[4]School of Energy and Chemical Engineering, Xiamen University Malaysia, Selangor Darul Ehsan 43900, Malaysia*
*[5]Department of Chemistry, Universitas Negeri Malang, Malang 65145, Indonesia.*
*[6]Center of Advanced Materials for Renewable Energy (CAMRY), Universitas Negeri Malang, Jl. Semarang No. 5, Malang 65145, Indonesia.*

*Received: 6th October 2025; Revised: 5th January 2026; Accepted: 7th January 2026*
*Available online: 13th January 2026; Published regularly: April 2026*

## Abstract

This paper presents the synthesis and characterization of calcium sulfate hemihydrate (CSH)-supported Metals (Ti, Fe, Cu or Ag) catalysts and their application in the styrene oxidation to benzaldehyde using hydrogen peroxide ($H_2O_2$) as an oxidant. The study explores the catalyst's structure-activity relationship, emphasizing the importance of mesoporous materials for enhanced catalytic performance. The CSH-Metals catalysts were synthesized using fish bone-derived CSH as a support, which aligns with green chemistry principles. Characterization techniques, such as FTIR, XRD, SEM, and BET surface area analysis, confirmed the successful impregnation of Metals (Ti, Fe, Cu or Ag) and its catalytic performance. The catalysts exhibited styrene conversion and high selectivity for benzaldehyde, achieving up to 49.5% and 60.2% for CSH-Ti; 12.9% and 84.1% for CSH-Fe, 19.9% and 61.5% for CSH-Cu, and 13.4% and 92.8% for CSH-Ag. The research highlights that the best catalyst's performance are CSH-Ti for styrene conversion and CSH-Ag for benzaldehyde selectivity. To support performance interpretation, a fuzzy logic analysis was applied to evaluate the influence of seven key parameters on catalytic behavior. The results revealed that ROS (Reactive Oxygen Species) formation activity, type of metal, and metal–intermediate interaction were the most dominant factors affecting performance. This data-driven insight reinforces the chemical reactivity as the primary determinant of catalyst effectiveness, above physical attributes such as surface area or pore structure. Overall, this study introduces a cost-effective, sustainable, and selective catalyst system for styrene oxidation, demonstrating high potential for industrial application in the production of value-added chemicals with minimal environmental impact.

***Keywords***: CSH-Metals; styrene oxidation; benzaldehyde; green chemistry; hydrogen peroxide; mesoporous materials

***How to Cite***: Rahmadani, A., Nurhadi, M., Wirawan, T., Wirhanuddin, W., Agusti, N. N., Lai, S. Y., Nur, H. (2026). Catalytic Performance of Environmentally Friendly Calcium Sulfate Hemihydrate-supported Metals (Ti, Fe, Cu or Ag) for Oxidation Styrene to Benzaldehyde. *Bulletin of Chemical Reaction Engineering & Catalysis*, 21 (1), 168-179. (doi: 10.9767/bcrec.20508)

***Permalink/DOI***: https://doi.org/10.9767/bcrec.20508

## 1. Introduction

The catalytic oxidation of styrene at its side chains is a topic of considerable interest in both academic research and industrial applications. This process yields valuable products such as styrene oxide and benzaldehyde, which serve as crucial and versatile synthetic intermediates in the chemical industry. Benzaldehyde, in particular, is a highly sought-after chemical with extensive applications in the manufacture of perfumery, anthelmintics, epoxy resins,

---

* Corresponding Author.
Email: nurhadi1969@yahoo.co.id (M. Nurhadi)

plasticizers, drugs, sweeteners, epoxy paints, pharmaceuticals, dyestuffs, and agrochemicals [1-4].

Traditionally, benzaldehyde can be synthesized through various routes, including benzyl alcohol oxidation, indirect electrochemical oxidation of toluene, benzoic acid hydrogenation, and benzyl chloride hydrolysis [5]. However, these conventional methods often present significant drawbacks. They typically involve high temperatures, prolonged reaction times, expensive starting materials, and the generation of copious and toxic waste, which is environmentally undesirable. Consequently, these methods frequently result in low catalytic conversion, poor benzaldehyde yields (often up to 20%), and limited selectivity [6].

In light of these challenges, styrene has emerged as an attractive alternative feedstock for benzaldehyde production. Its large-scale industrial availability, relatively low cost, and compatibility with selective oxidation pathways make it a promising raw material [7,8]. Styrene is predominantly produced from ethylbenzene, a major petrochemical commodity with a global annual production exceeding 30 million tons, ensuring its abundant and reliable supply [8]. Furthermore, recent advances have demonstrated the potential of bio-based styrene derived from renewable lignocellulosic resources, reinforcing its growing relevance as a more sustainable feedstock for value-added oxidation processes. These aspects underscore the critical need for developing environmentally benign and efficient catalytic systems for the selective oxidation of styrene to benzaldehyde [9].

Many researchers have endeavored to develop ideal preparation methods that can enhance the controllable conversion of styrene to benzaldehyde using catalysts [10]. Direct oxidation of styrene with air or oxygen as the oxidant, in the presence of various homogeneous and heterogeneous catalysts, is considered the most ideal approach [11-14]. However, homogeneous catalysts face major limitations, such as high costs, difficulties in catalyst separation from the reaction mixture, poor recycling performance, and in some cases, rather low catalytic activities. Moreover, most homogeneous catalysts become inactive after reaction, rendering them unsuitable for industrial applications. Consequently, heterogeneous catalysts have gained significant attention and have been successfully developed for styrene oxidation due to their efficiency, ease of separation, reusability, and environmental friendliness, aligning with green chemistry principles. Effective heterogeneous catalysts require metals that exhibit high redox activity, surface stability, efficient oxygen activation, and strong metal–support interactions to promote selective oxidation reactions [15-17]. Recently, inexpensive transition metals, such as Ti, Fe, Cu, and Ag, have attracted considerable attention as promising alternatives to noble metals due to their ability to generate reactive oxygen species, good thermal stability, and lower toxicity and cost [18–21]. It is important to note that, unlike noble metals, not all metals are equally suitable as heterogeneous catalysts, and their effectiveness strongly depends on their electronic structure, oxidation states, and interaction with the catalyst supports [22-24].

Despite extensive research on various heterogeneous catalysts for styrene oxidation using $H_2O_2$ as an oxidant-including $TiO_2$ [25], Co–ZSM-5 [5], Fe-SBA-15 [26], $Ce_xCo_{1-x}Fe_2O_4$ [27], Ag-$WO_3$ [28], $NiCo_2O_4$ and Co(Ni)$PW_{12}$ [29], Ag-ferrite [30], $V_2O_5$/g-$C_3N_4$ [31], Spherical V-MCM-48[32], ZnPc–MWCNTs [33], Ni–Gd ferrites [34], Fe- and Ti-SBA-1 [35], Mg–Co–Al hydrotalcite [36], Mg–Cu ferrite [37], Ag-Co-MCM-41 [38] $H_3PW_{12}O_{40}$ on SBA-15 [39], many of these systems still suffer from significant drawbacks. Specifically, they often rely on expensive catalyst supports and active sites, and their overall processes are not always environmentally friendly. This highlights a persistent and critical gap in the field: the need for efficient, selective, cost-effective, and truly environmentally benign catalytic systems, particularly those derived from sustainable and waste resources.

In this context, the present study introduces a novel approach by utilizing Calcium Sulfate Hemihydrate (CSH) derived from fish bone waste as a sustainable and low-cost support for various transition metals (Titanium, Iron, Copper, or Silver). The selection of CSH from fish bone waste is scientifically justified by both its material functionality and sustainability considerations [7,40-44]. Fish-bone derived materials possess surface $Ca^{2+}$ sites and surface hydroxyl/sulfate groups that act as anchoring and coordination sites for metal oxides and metallic nanoparticles, facilitating high dispersion and strong metal–support interactions. Thermal and chemical processing of bones typically produces porous matrices with appreciable surface area and tunable acid–base properties, which improve mass transport and promote the generation/activation of reactive oxygen species (ROS) from oxidants like $H_2O_2$ on the catalyst surface. Furthermore, from an ecological perspective, the goal of this research is to develop efficient catalytic methods that produce compounds with both atom-saving and environmental benefits. Considering oxidation reactions with oxygen donors, the use of catalytic oxygen transfer-based technologies from clean oxygen donors, such as hydrogen peroxide ($H_2O_2$) is highly preferred. Oxidation using $H_2O_2$ as an oxidant is motivated by its ease of handling, high active oxygen content, and the fact that water is the only by product, making it an environmentally benign approach [25].

## 2. Materials and methods

### 2.1 Fabrication of CSH

The procedure of CSH fabrication was carried out following the previous research [7,40]. Every 1 gram carbon from fishbone was mixed with 6 mL of concentrated sulfuric acid ($H_2SO_4$; JT Beker). The mixture was stirred at room temperature for 3 h and washed with distillate water to remove any loosely bound acid until pH of filtrate 2. Then, the carbon solution was saved at room temperature for few days until the crystal growth. Furthermore, decantation and filtration were conducted to separate carbon and crystal. The crystal was washed until the filtrate reached neutral pH. The crystal then dried at 110 °C for overnight.

### 2.2 Metals Impregnation

The materials that used in the impregnation process such as CSH, Titanium(IV) isopropoxide (Sigma Aldrich), Iron(III) nitrate (Merck), Copper(II) nitrate (Merck) and Silver nitrate (Merck), Ethanol (Merck) and Acetone (Merck). The impregnation method follows the previous research [11]. Firstly, the CSH crystal was crushed until the size 200 mesh. The 1 g CSH was impregnated by metals 500 μmol that was immersed in 10 mL acetone (Merck) and stirred until all of the acetone solvents completely evaporated. The residual acetone was removed from the CSH sample by washing with ethanol (Merck) and subsequently dried at 110 °C overnight. The CSH sample was impregnated and labeled as CSH-M, M = Ti, Fe, Cu or Ag. For example, CSH-Ti was the CSH that was impregnated by titanium(IV) isopropoxide (500 μmol).

Table 1. Elements analysis of CSH-Ti, CSH-Cu, CSH-Fe and CSH-Ag obtained using WDXRF.

| Element (wt%) | CSH-Ti | CSH-Cu | CSH-Fe | CSH-Ag |
|---|---|---|---|---|
| Mg | 4.0 | - | - | 3.0 |
| P | 0.49 | - | 0.41 | 0.20 |
| S | 26.9 | 26.8 | 25.5 | 19.2 |
| Ti | 8.34 | - | - | - |
| Ca | 59.6 | 59.1 | 61.5 | 56.9 |
| Fe | 0.059 | 0.089 | 11.7 | 0.067 |
| Cu | 0.055 | 13.1 | 0.057 | 0.046 |
| Ag | - | - | - | 12.4 |
| Sr | 0.24 | 0.43 | 0.37 | 0.24 |
| Yb | 0.15 | 0.27 | 0.25 | 0.17 |

### 2.3 Samples Characterization

A series of catalysts, such as CSH-Ti, CSH-Fe, CSH-Cu and CSH-Ag, were characterized by using Wavelength Dispersive X-Ray Fluorescence Spectroscopy (WDXRF), Fourier Transform Infra Red (FTIR), X-ray Diffraction (XRD), Scanning Electron Microscopy (SEM) and $N_2$ adsorption-desorption to investigate the structure-activity relationships between the catalysts and the styrene oxidation. WDXRF (PANalytical, Minipal 4) was used to determine the chemical composition from the catalyst. The functional groups in the catalyst were investigated by using FTIR spectrometer (IR−Prestige−21 Shimadzu). XRD instrument (Philips PANalytical X'Pert PRO) was used to investigate the crystallinity and phase content of the catalysts. SEM-EDX (FEI Inspect S50) instrument was used to determine the surface morphology and element containing the catalyst. The surface area, pore volume and pore size of the catalyst were determined by using the nitrogen adsorption-desorption instrument (Quantachrome NovaWIn instrument version 11.0).

### 2.4 Catalyst Performance Test

The catalyst performance was tested for a styrene oxidation reaction with hydrogen peroxide ($H_2O_2$, Merck) as an oxidant. The reactions procedure was carried out following the previous research [11,45]. All reactions were carried out for 24 h at room temperature with reacting 5 mmol styrene (Merck), 5 mmol aqueous $H_2O_2$ (Merck), 4.5 mL acetonitrile (Merck), and 100 mg catalyst under stirring. The reaction products were withdrawn and analyzed by GC-2010 Shimadzu-gas chromatograph equipped with a SH-Rxi-5ms column (30 m × 0.25 mmID × 0.25 μm df), serial 1652111, a flame ionization detector (FID) and nitrogen as the carrier gas. The GC method: the temperatures of the injector and detector were programmed at 250 and 260 °C, respectively; the temperature of the column oven was programmed at 80 °C; pressure 100 kPa; flow 28 mL/min; collumb flow 1.19 mL/min; linear velocity 31.1 cm/s; purge flow 3.0 mL/min; spit ration 20.

## 3. Results and discussion

### 3.1. Physical Properties

The elements present in CSH-Ti, CSH-Cu, CSH-Fe, and CSH-Ag were determined using wavelength dispersive X-ray fluorescence (WDXRF). The complete results of the elemental analysis are shown in Table 1. All catalysts consists primarily of calcium (Ca) and sulfur (S) as major elements. Various metal elements were also found within the catalysts, such as magnesium (Mg), phosphor (P), strontium (Sr) and ytterbium (Yb). The impregnation of metals

(Ti, Cu, Fe and Ag) are evidenced by the percentage of titanium (8.34%) in CSH-Ti; cuprum (13.1%) in CSH-Cu; ferrum (11.7%) in CSH-Fe; and argentum (12.4%) in CSH-Ag.

Figure 1 shows the FTIR spectra of (a) CSH, (b) CSH-Ti, (c) CSH-Fe, (d) CSH-Cu, and (e) CSH-Ag that measured over the range of 400–4000 cm$^{-1}$. The O–H stretching that might be attributed to adsorbed water molecules appear in all spectra on absorption peaks around 3200–3600 cm$^{-1}$. The CSH crystal was investigated by absorption bands at 3613, 3559, and 1687 cm$^{-1}$, associated with crystal water molecules combined in $CaSO_4$ [46-48]. The characteristic bands of $CaSO_4$ can be identified by the band at 1272 cm$^{-1}$, assigned to $Ca^{2+}$, and bands at 1108, 1007, 673, and 618 cm$^{-1}$, assigned to $SO_4^{2-}$ stretching. Figure 1 (b-e) show FTIR spectra after the impregnation of metals (Ti, Fe, Cu and Ag). The absorption peaks due to metal impregnation can be observed in Figure 1 (b-e). The presence of titania in the catalyst samples is evidenced by absorption peaks around 900–1000 cm$^{-1}$, which indicate the local stretching modes of [$TiO_4$] and/or [$O_3TiOH$], and the titanyl [Ti=O] vibration [49-51]. The presence of copper in the catalyst samples is identified by absorption peaks around 420–624 cm$^{-1}$. The existence of iron in the catalysts samples is investigated by absorption peaks around 570–580 cm$^{-1}$. The metal of silver in the samples is evidenced by absorption peaks around 585–620 cm$^{-1}$. However, the absorption band of Ti–O, Cu–O, Fe–O, and Ag–O in these FTIR spectra are indistinct, which are attributed to the small amount of metals impregnated onto CSH.

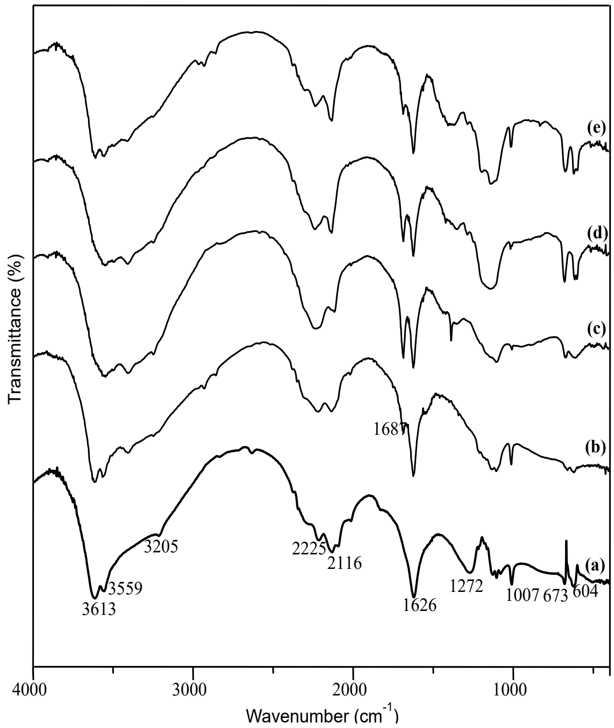

Figure 1. FTIR spectra of (a) CSH, (b) CSH-Ti, (c) CSH-Fe, (d) CSH-Cu, and (e) CSH-Ag.

Figure 2 shows the XRD patterns illustrating the crystallinity of (a) $TiO_2$, (b) CSH, (c) CSH-Ti, (d) CSH-Fe, (e) CSH-Cu, and (f) CSH-Ag catalysts. Figure 2(a) displays the $TiO_2$ catalyst, as evidenced by diffraction peaks at 2θ = 25.2°, 37.7°, 47.9°, 53.7°, and 55.1°. Figure 2(b) shows the CSH catalyst, identified by diffraction peaks at 2θ = 14.7°, 25.7°, 29.7°, 31.9°, 42.2°, and 49.4°. Figures 2(c) show CSH impregnated with Ti, as proven by the dominant diffraction peaks at 2θ = 14.7° and 25.7° for CSH, and 2θ = 25.2° and 37.7° for titania. Figures 2(d) show CSH impregnated with Fe, identified by main characteristic diffraction peaks at 2θ = 30.1° and 43.1°. Figures 2(e) show CSH impregnated with Cu, identified by diffraction peaks at 2θ = 36.37° and 42.26°, matched well with JCPDS No. 1000063. Figures 2(f) show CSH impregnated with Ag, identified by main characteristic diffraction peaks at 2θ = 38.1°, and 44.3° and can be indexed as the cubic phase of Ag (JCPDS No. 04-0783).

Figure 3 exhibits the SEM images of catalysts (a) CSH-Ti, (b) CSH-Fe, (c) CSH-Cu, and (d) CSH-Ag. All catalysts show roughened surfaces due to metal deposition. The rough surface morphology observed in the SEM images

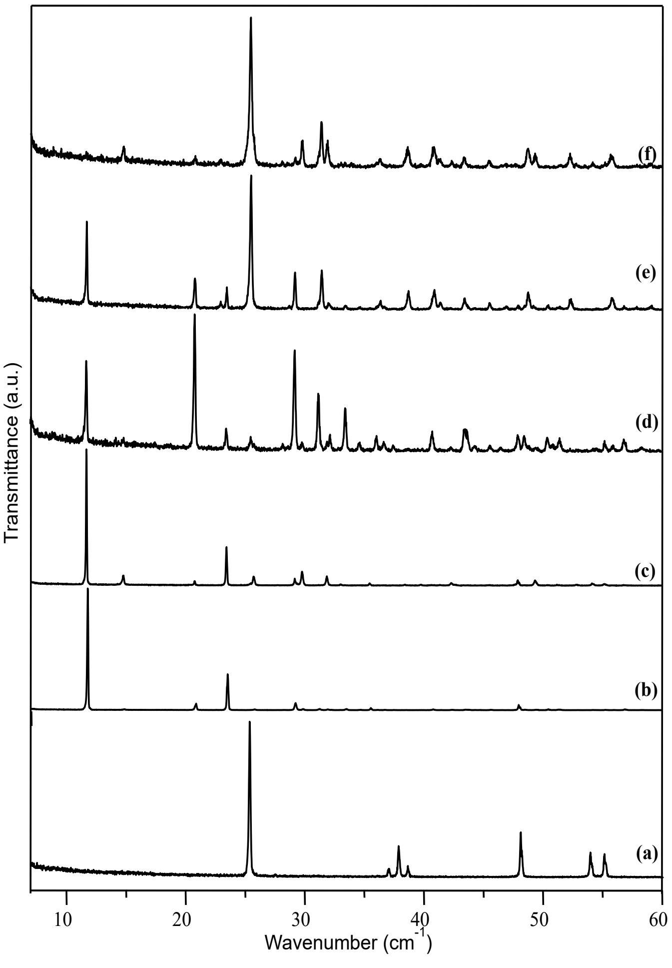

Figure 2. XRD pattern of (a) $TiO_2$, (b) CSH, (c) CSH-Ti, (d) CSH-Fe, (e) CSH-Cu, and (f) CSH-Ag.

suggests an increase in the active surface area, facilitating more efficient contact between the catalyst and the styrene molecules. This enhanced surface area allows for a higher conversion rate as more reactant molecules interact with the catalyst's active sites. Figure 3 (a) and (c) show are not only rough surface morphology also appear small particle size. Figure 3(b) was identified rough surface morphology, big particles size and cubic shaped particles. Figure 3(d) besides the rough surface morphology also needle-shaped particles.

Nitrogen adsorption-desorption analysis was used to determine the BET surface area, pore volume, and mean pore size of CSH-Ti, CSH-Fe, CSH-Cu, and CSH-Ag. Figure 4 shows the isotherms for (a) CSH-Ti, (b) CSH-Fe, (c) CSH-Cu, and (d) CSH-Ag, which exhibit type IV isotherms according to IUPAC classification, with narrow hysteresis loops. The isotherms display narrow hysteresis loops in the relative pressure range of approximately 0.6–1.0 for CSH-Ti, 0.45–1.0 for CSH-Fe, 0.65–1.0 for CSH-Cu and 0.45–1.0 for CSH-Ag. The isotherms also display the knee shape which shows the presence of meso-sized pores. The pore size distribution of all samples is between 2 nm and 50 nm, indicating the presence

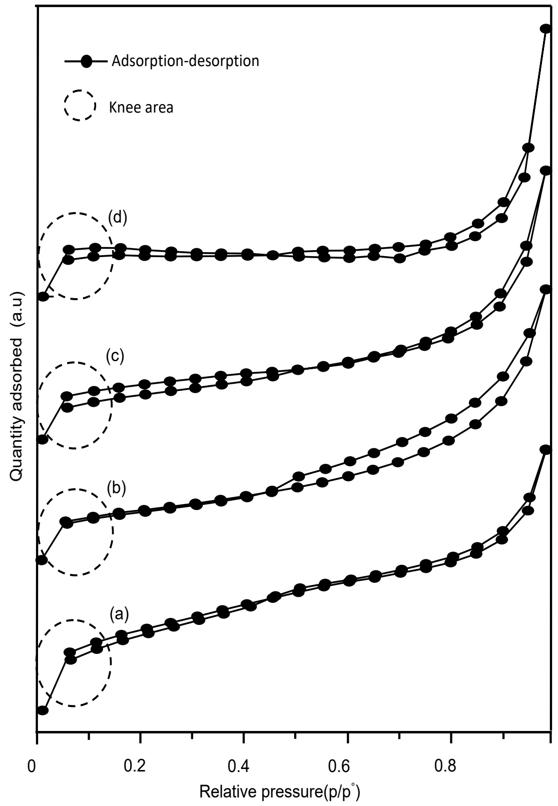

Figure 4. The physisorption isotherms of (a) CSH-Ti, (b) CSH-Fe, (c) CSH-Cu, and (d) CSH-Ag.

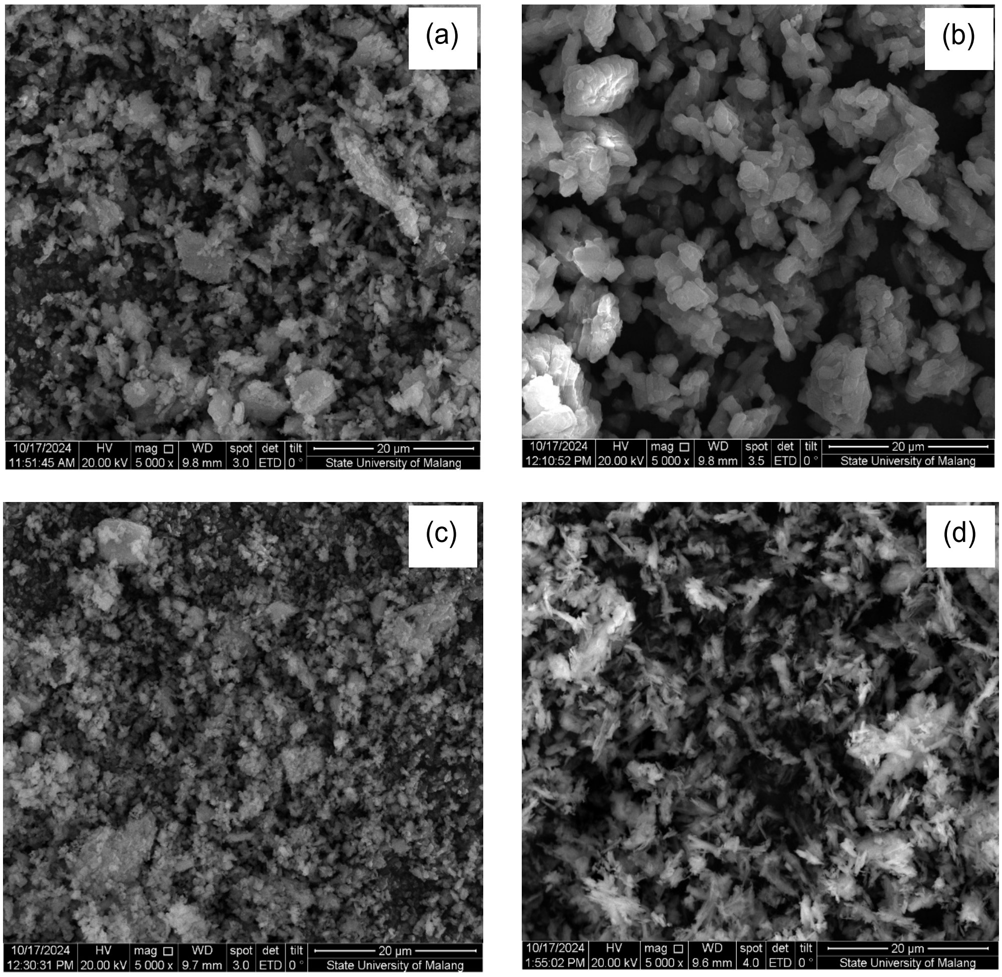

Figure 3. SEM Image of (a) CSH-Ti, (b) CSH-Fe, (c) CSH-Cu, and (d) CSH-Ag.

of uniform mesopores. The BET surface area and pore volume showed the following values: CSH (11.33 $m^2/g$, 0.043 $cm^3/g$), CSH-Ti (21.99 $m^2/g$, 0.0304 $cm^3/g$), CSH-Fe (23.37 $m^2/g$, 0.0561 $cm^3/g$), CSH-Cu (12.89 $m^2/g$, 0.0284 $cm^3/g$), and CSH-Ag (3.96 $m^2/g$, 0.0128 $cm^3/g$). The complete data are listed in Table 2.

### 3.2. Catalytic Activity

#### 3.2.1 Catalysis

After the successful incorporation of metals into the CSH, the material was employed as a catalyst for the classical oxidation of styrene, as depicted in Scheme in Figure 5. Catalysts, such as $TiO_2$, CSH, CSH-Ti, CSH-Fe, CSH-Cu, and CSH-Ag, were tested in the oxidation of styrene using $H_2O_2$ as the oxidant. The products of styrene oxidation using $H_2O_2$ were benzaldehyde, phenylacetaldehyde, styrene oxide, and others, with benzaldehyde being the dominant product. The formation of benzaldehyde was started from the nucleophilic attack of $H_2O_2$ on styrene oxide, followed by cleavage of the intermediate hydroxy–hydroperoxystyrene, oxygen transfer from metallic oxides to styrene, and finally cleavage of the metalloepoxy intermediate and the C=C bond [52-53]. In this study, benzaldehyde was the main product when using CSH, CSH-Ti, CSH-Fe, CSH-Cu, and CSH-Ag catalysts, with selectivity around 61–93%. When CSH was used as a catalyst, the conversion was 5.8% with styrene oxide as the main product, and the selectivity was about 65%. This conversion was slightly higher than when without catalyst. The complete yields and product selectivities for the oxidation of styrene with $H_2O_2$ as the oxidant are shown in Table 3.

Table 2. Physical properties of the samples.

| Samples | BET surface area ($m^2/g$) | Pore Volume ($cm^3/g$) | Mean pore size (nm) |
|---|---|---|---|
| CSH | 11.336 | 0.0428 | 7.5 |
| CSH-Ti | 21.986 | 0.0304 | 2.7 |
| CSH-Fe | 23.366 | 0.0561 | 4.8 |
| CSH-Cu | 12.895 | 0.0284 | 4.4 |
| CSH-Ag | 3.965 | 0.0128 | 6.4 |

$H_2O_2$ was chosen as the oxidant in this process due to its environmentally friendly nature. Upon decomposition, $H_2O_2$ produces only water and oxygen, avoiding the formation of harmful by-products typically associated with other oxidants. This makes $H_2O_2$ an ideal oxidant for green chemistry applications, ensuring that styrene oxidation proceeds with minimal environmental impact while maintaining high selectivity for the desired product, benzaldehyde. $H_2O_2$ acts as an effective oxidant in this reaction due to its ability to decompose into reactive oxygen species (ROS) on the metals catalyst surface. The interaction between $H_2O_2$ and metals ion species ($Ti^{3+}/Ti^{4+}$; $Fe^{2+}/Fe^{3+}$; $Cu^{+}/Cu^{2+}$ or $Ag^{+}$) on the catalyst surface facilitates homolytic cleavage of the O–O bond, generating hydroxyl radicals (•OH) and hydroperoxy radicals (•OOH), which promote the oxidation of styrene. This

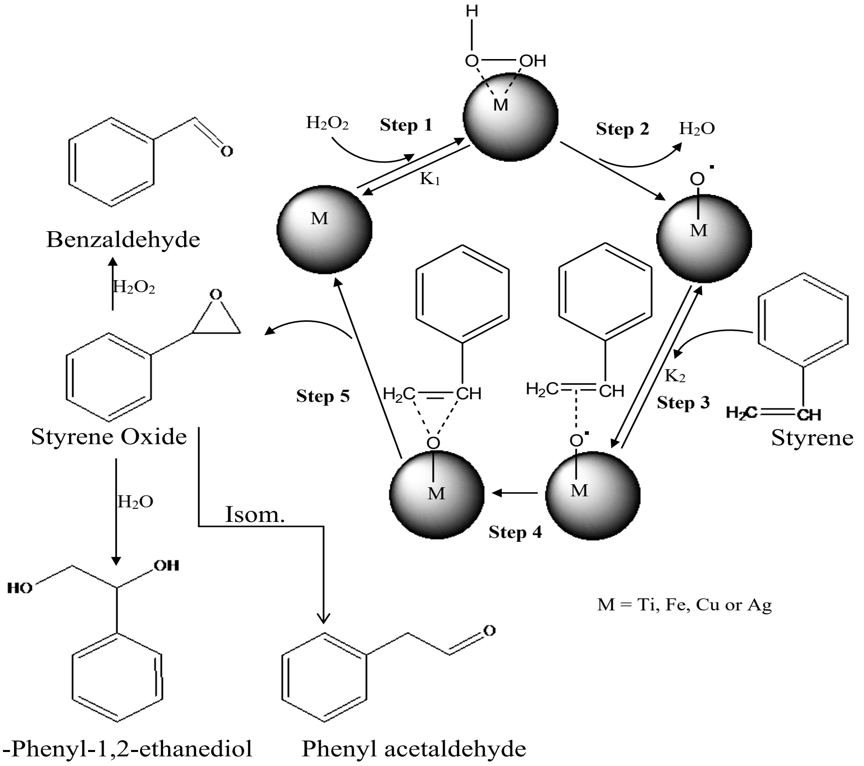

Figure 5. Reaction scheme of the styrene oxidation with $H_2O_2$ as oxidant [54-55].

interaction allows the oxidation to occur under mild conditions, making $H_2O_2$ a highly efficient and environmentally friendly oxidant for this process. The high selectivity for benzaldehyde observed in styrene oxidation can be attributed to the surface properties of the CSH metal catalyst. The presence of acidic sites on metal promotes the cleavage of the C=C bond and the epoxide ring, favoring the formation of benzaldehyde rather than styrene oxide or phenylacetaldehyde. In addition, the dispersion of metal particles on the CSH support increases the accessibility of the active sites, ensuring that the oxidation process proceeds efficiently with minimal formation of by-products.

The conversions of styrene over no catalyst, CSH, CSH-Ti, CSH-Fe, CSH-Cu, and CSH-Ag catalysts were 1.43%, 5.86%, 49.45%, 12.86%, 19.93%, and 13.40%, respectively. Reactions without catalyst and using only CSH as catalysts occurred at a very low rate. The role of the catalyst support is demonstrated by comparing the styrene conversions using CSH, CSH-Ti, CSH-Fe, CSH-Cu, and CSH-Ag as catalysts. The styrene oxidation using the support catalyst (CSH) showed lower activity than metals (Ti, Fe, Cu and Ag) supported on CSH (CSH-Ti, CSH-Fe, CSH-Cu, and CSH-Ag). CSH-Ti and CSH-Cu have the high catalytic activity but their benzaldehyde selectivity is low (~60%). It was caused the styrene oxide as intermediate product in styrene oxidation not only convert to benzaldehyde but also directly convert to another products, such as phenyl acetaldehyde and 1-phenyl 1,2 etanediol. Otherwise, CSH-Fe and CSH-Ag have high benzaldehyde selectivity (~90%). It was caused the styrene oxide as intermediate product in styrene oxidation directly convert to benzaldehyde. The styrene oxidation mechanism can be shown in Figure 5.

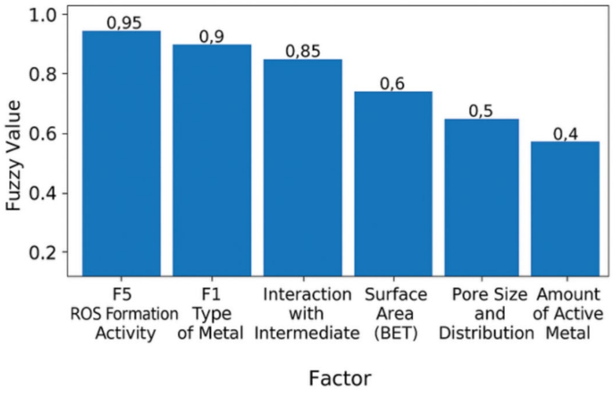

Figure 6. The fuzzy membership values for seven key catalytic parameters. ROS formation activity (F5) exhibits the highest influence, followed by metal type (F1) and intermediate interaction (F6).

It should be noted that the moderate styrene conversion observed in this study is mainly associated with the deliberately mild reaction conditions employed, namely room temperature operation and the use of hydrogen peroxide as a green oxidant. In contrast to many reported styrene oxidation systems that rely on elevated temperatures, pressurized conditions, or strong oxidants, the present work prioritizes selectivity, catalyst stability, and environmental compatibility in line with green chemistry principles.

A comparison between catalytic performance and the physical properties listed in Table 2 indicates that styrene conversion does not exhibit a linear correlation with BET surface area, pore volume, or mean pore diameter. For instance, CSH-Fe exhibits the highest BET surface area among the catalysts studied, yet its styrene conversion is considerably lower than that of CSH-Ti. Conversely, CSH-Ag possesses the lowest surface area but achieves the highest benzaldehyde selectivity. These observations suggest that textural properties alone are insufficient to explain the observed catalytic trends.

The presence of metals oxide in the catalyst, confirmed by absorption bands around 900–1000 $cm^{-1}$ for TiO2; around 420–624 $cm^{-1}$ for CuO; around 570–580 $cm^{-1}$ for $Fe_3O_4$ and around 585–620 $cm^{-1}$ for $Ag_2O$ (see FTIR spectra in Figure 1), is associated with the formation of reactive oxygen species (ROS), such as hydroxyl radicals (•OH) and hydroperoxy radicals (•OOH). These species are crucial in enhancing the catalytic activity of CSH-Metals by promoting the oxidation of

Table 3. Catalytic performance of the catalysts in the oxidation of styrene[a].

| Catalyst | Conversion (%) | Selectivity (%) | | | |
|---|---|---|---|---|---|
| | | BzA[b] | PhA[c] | SO[d] | Other |
| No catalyst | 1.43 | 25.19 | 0 | 41.05 | 33.75 |
| CSH | 5.80 | 18.07 | 1.59 | 65.21 | 15.13 |
| CSH-Ti | 49.45 | 60.21 | 0.71 | 0.69 | 38.39 |
| CSH-Fe | 12.86 | 84.08 | 6.89 | - | 9.02 |
| CSH-Cu | 19.93 | 61.45 | 5.75 | 20.12 | 12.66 |
| CSH-Ag | 13.40 | 92.81 | - | - | 7.18 |

[a] Reaction conditions: The reactions were carried out at room temperature for 24 h with styrene (5 mmol), 30% $H_2O_2$ (5 mmol), and catalyst (100 mg). BzA[b] = benzaldehyde, PhA[c] = phenylacetaldehyde, and SO[d] = styrene oxide

styrene, thereby increasing the conversion and selectivity toward benzaldehyde. The catalytic oxidation of styrene over CSH-Metals is driven by the generation of reactive oxygen species (ROS) on the titania surface. When $H_2O_2$ is introduced, it decomposes into hydroxyl radicals (•OH) and hydroperoxy radicals (•OOH), which are highly reactive and capable of initiating the oxidation of styrene. These ROS facilitate the nucleophilic attack on the C=C bond of styrene, leading to the formation of styrene oxide, which subsequently undergoes cleavage to produce benzaldehyde. The presence of these ROS on the catalyst surface enhances the overall catalytic efficiency and selectivity for benzaldehyde. The oxidation of styrene begins with the formation of styrene oxide, acting as an intermediate. The nucleophilic attack of reactive oxygen species (•OH and •OOH) on the epoxide ring leads to the cleavage of the C=C bond, ultimately resulting in the formation of benzaldehyde. The selective formation of benzaldehyde can be attributed to the ability of the titania catalyst to stabilize the intermediate and direct the reaction toward the cleavage of the metalloepoxy intermediate, which favors the production of benzaldehyde over other side products such as phenylacetaldehyde or styrene oxide. These results imply that catalytic performance in the present system is governed predominantly by chemical factors rather than by surface area or pore-related properties alone, necessitating a systematic evaluation of multiple contributing parameters.

### 3.3. Fuzzy Logic Analysis of Dominant Factors Affecting Catalytic Performance

To elucidate the relative importance of the various factors influencing catalytic performance, a semi-quantitative fuzzy logic analysis was employed. This approach allows the evaluation of interdependent parameters when direct linear correlations between physical properties and catalytic activity are not evident. The fuzzy logic results clearly indicate that chemical factors, particularly the redox behavior of the supported metal species and their ability to generate reactive oxygen species (ROS) from $H_2O_2$, play a dominant role in determining styrene conversion and benzaldehyde selectivity. In contrast, physical properties such as surface area, pore size distribution, and morphology contribute in a secondary manner. This finding is consistent with the experimental observations discussed in Section 3.2.1 and explains why catalysts with lower surface area can still exhibit superior catalytic performance.

To further analyze and rank the dominant factors contributing to the catalytic oxidation of styrene, a fuzzy logic-based assessment was conducted. This method allows semi-quantitative evaluation of various interrelated parameters, particularly when their effects on catalytic performance are overlapping or nonlinear. Seven primary variables were identified from the experimental data and catalyst characterizations: (1). F1 – Type of Metal (Ti, Fe, Cu, Ag); (2). F2 – Surface Area (BET); (3). F3 – Pore Size and Distribution; (4). F4 – Surface Morphology (SEM); (5). F5 – ROS (Reactive Oxygen Species) Formation Activity; (6). F6 – Interaction with Reaction Intermediate; (7). F7 – Amount of Active Metal. Each factor was assigned a fuzzy membership value in the range 0–1, based on observed influence on styrene conversion and selectivity toward benzaldehyde. The membership levels were categorized into linguistic terms: Low (0.00–0.30), Medium (0.31–0.69), and High (0.70–1.00). The fuzzy evaluation of factor influencing catalytic activity was listed in Table 4.

The fuzzy logic analysis revealed substantial differences in the relative contributions of various parameters to the catalytic performance of the CSH-metal systems. Figure 6 clearly illustrates that ROS (Reactive Oxygen Species) formation

Table 4. Fuzzy evaluation of factors influencing catalytic activity.

| Factor Code | Description | Fuzzy Value | Linguistic Level | Justification |
|---|---|---|---|---|
| F5 | ROS Formation Activity | 0.95 | High | Major source of oxidation reactivity via radical generation from $H_2O_2$ |
| F1 | Type of Metal | 0.90 | High | Strongly influences both conversion and selectivity due to redox behavior |
| F6 | Interaction with Intermediate | 0.85 | High | Affects pathway selectivity to benzaldehyde over side-products |
| F2 | Surface Area (BET) | 0.70 | High | Higher surface allows more exposed active sites |
| F4 | Surface Morphology | 0.60 | Medium | Rougher surface enhances contact but not dominant |
| F3 | Pore Size and Distribution | 0.50 | Medium | Mesoporosity assists diffusion; effect relatively uniform across catalysts |
| F7 | Amount of Active Metal | 0.40 | Medium | Not linearly related to performance; dispersion is more critical |

activity (F5) is the most dominant factor, with a fuzzy membership value of 0.95, highlighting its critical role in initiating and sustaining the oxidation of styrene via the formation of highly reactive radicals such as •OH and •OOH. In addition, Figure 6 also shows that the type of metal used (F1) and the interaction with reaction intermediates (F6) are the second and third most influential factors, with fuzzy values of 0.90 and 0.85, respectively. These factors significantly affect both the conversion efficiency and product selectivity by governing the redox behavior of the catalyst and directing the reaction pathway toward benzaldehyde, the desired oxidation product.

In contrast, physical parameters such as BET surface area (F2) and surface morphology (F4) showed moderate influence, while pore size distribution (F3) and the amount of metal loading (F7) contributed less significantly to overall performance. Although these structural features are important for enhancing diffusion and active site accessibility, they are not as critical as the chemical factors that control electron transfer and intermediate transformation. This analysis underscores that chemical reactivity, especially the catalyst's ability to generate ROS and interact with key intermediates, is the primary determinant of catalytic success in the oxidation of styrene.

Accordingly, fuzzy logic provides a clear hierarchy of design priorities, the detailed methodology and worked calculations of which are provided in the Supplementary Information (S1). To optimize catalyst performance under green chemistry principles, attention should focus on: Enhancing ROS formation efficiency; Selecting the appropriate metal species with favorable redox properties; and Facilitating strong metal–substrate interactions. These three factors offer the most leverage for improving both conversion and selectivity, supporting the development of highly effective, environmentally benign catalytic systems.

## 4. Conclusions

This study successfully developed a series of environmentally friendly heterogeneous catalysts consisting of calcium sulfate hemihydrate (CSH) derived from fish bone waste as a sustainable support for transition metals (Ti, Fe, Cu, and Ag) and demonstrated their applicability in the selective oxidation of styrene using hydrogen peroxide ($H_2O_2$) as a green oxidant. Comprehensive characterization confirmed the successful formation of metal supported CSH catalysts with preserved crystalline structure and mesoporous characteristics, providing adequate accessibility to active sites under mild reaction conditions. Catalytic evaluation showed that all synthesized catalysts were active for styrene oxidation, achieving benzaldehyde selectivities of up to 93%. Among the catalysts investigated, CSH-Ti exhibited the highest styrene conversion, whereas CSH-Ag delivered the highest selectivity toward benzaldehyde, highlighting the distinct roles of metal species in controlling reaction pathways. These results demonstrate that high selectivity and effective catalytic performance can be achieved without relying on noble metals or synthetic supports, emphasizing the potential of waste derived CSH as a cost effective and sustainable alternative. To elucidate the structure activity relationship, a semi quantitative fuzzy logic analysis was employed to assess the relative influence of multiple catalytic parameters. The analysis revealed that chemical factors, particularly reactive oxygen species formation activity, metal type, and interactions between metal sites and reaction intermediates, play a dominant role in governing catalytic efficiency and selectivity, whereas physical properties such as surface area and morphology contribute in a secondary manner. Overall, this work provides valuable insights into the design of sustainable oxidation catalysts and underscores the importance of chemically driven mechanisms over purely textural properties in styrene oxidation reactions.

## Acknowledgment

The authors gratefully acknowledge research grant *Direktorat Jenderal Riset dan Pengembangan, Kementerian Pendidikan Tinggi, Sains dan Teknologi Tahun Anggaran* 2025 by contract number: 554/UN17.L1/HK/2025.

## CRedit Author Statement

Author Contributions: A. Rahmadani: Conceptualization, Methodology, Investigation, Resources, Data Curation, Writing, Writing Draft Preparation; M. Nurhadi: Conceptualization, Methodology, Investigation, Resources, Data Curation, Writing, Review and Editing, Supervision; T. Wirawan: Conceptualization, Methodology, Investigation, Resources, Data Curation, Writing, Writing Draft Preparation. Wirhanuddin: Data Curation and Project Administration; N. N Agusti: Data Curation and Project Administration; S. Y. Lai : Proofreading, Writing, Review and Editing.; H. Nur: Proofreading, Writing, Review and Editing. All authors have read and agreed to the published version of the manuscript.

## References

[1] Xie, L., Wang, H., Lu, B., Zhao, J., Cai, Q. (2018). Highly selective oxidation of styrene to benzaldehyde over Fe3O4 using H2O2 aqueous solution as oxidant. *React. Kinet. Mechan. Catal.* 125(2), 743–756. DOI: 10.1007/s11144-018-1429-6

[2] Aberkouks, A., Mekkaoui, A.A., Boualy, B., Houssame, S.E., Ali, M.A., Firdoussi, L.E. (2018). Selective Oxidation of Styrene to Benzaldehyde by Co-Ag Codoped ZnO Catalyst and H2O2 as Oxidant. *Adv. Mater. Sci. Eng.* 1-7. DOI: 10.1155/2018/2716435

[3] Qi, B., Lu, X.H., Zhou, D., Xia, Q.H., Tang, Z.R., Fang, S.Y., Pang, T., Dong, Y.L., (2010). Catalytic epoxidation of alkenes with 30% H2O2 over Mn2+-exchanged zeolites. *J. Mol. Catal. A: Chem.*, 322(1–2), 73-79. DOI: 10.1016/j.molcata.2010.02.019

[4] Zhan, W., Guo, Y., Wang, Y., Guo, Y., Liu, Y.X., Wang, Y., Zhang, Z., Lu, G. (2009), Study of Higher Selectivity to Styrene Oxide in the Epoxidation of Styrene with Hydrogen Peroxide over La-Doped MCM-48 Catalyst. *J. Phys. Chem. C*, 113(17), 7181-7185. DOI: 10.1021/jp8101095

[5] Pierella, L.B., Saux, C., Caglieri, S.C., Bertorello, Hc.R., Bercoff, P.G. (2008) Catalytic activity and magnetic properties of Co–ZSM-5 zeolites prepared by different methods. *Appl. Catal. A: Gen.* 347, 55–61. DOI: 10.1016/j.apcata.2008.05.033

[6] Zhu, X., Shen, R., Zhang, L. (2014) Catalytic oxidation of styrene to benzaldehyde over a copper Schiff-base/SBA-15 catalyst. *Chinese J. Catal.* 35, 1716–1726. DOI: 10.1016/S1872-2067(14)60131-5

[7] Koesnarpadi, S., Wirawan, T., Nurhadi, M., Wirhanudin, W., Prananto, Y.P., Nazarudin, N., Volkan Degirmenci, V., Lai, S.Y., Nur, H. (2024) Oxidation of Styrene to Benzaldehyde Using Environmentally Friendly Calcium Sulfate Hemihydrate-Supported Titania Catalysts. *Bull. Chem. React. Eng. Catal.*, 19(4), 622-634. DOI: 10.9767/bcrec.20224

[8] World Health Organization (WHO). (2020). Styrene. In: Some industrial chemicals. Geneva: World Health Organization

[9] Fan, G., Zhu, B., Lei, Y., Zhang, Z., Ma, J., Chen, Y. (2026). Biomass-based styrene production: Process design, techno-economic analysis and life cycle assessment. *Chem. Eng. Sci.*, 320(A), 122460. DOI: 10.1016/j.ces.2025.122460

[10] Xie, L., Wang, H., Lu, B., Zhao, J., Cai, Q. (2018). Highly selective oxidation of styrene to benzaldehyde over Fe3O4 using H2O2 aqueous solution as oxidant. *React. Kinet., Mechan. Catal.*. 125(2), 743-756. DOI: 10.1007/s11144-018-1429-6

[11] Nurhadi, M., Kusumawardani, R., Wirawan, T., Sumari, S., Yuan, L.S., Nur, H., (2021) Catalytic Performance of TiO2–Carbon Mesoporous_Derived from Fish Bones in Styrene Oxidation with Aqueous Hydrogen Peroxide as an Oxidant. *Bull. Chem. React. Eng. Catal.*, 16(1), 88-96. DOI: 10.9767/bcrec.16.1.9729.88-96

[12] Liu, L., He, W., Fang, Z., Yang, Z., Guo, K., Wang, Z. (2020), From Core−Shell to Yolk−Shell: Improved Catalytic Performance toward CoFe2O4@ Hollow@ Mesoporous TiO2 toward Selective Oxidation of Styrene. *Indust. Eng. Chem. Res.*, 59(45), 19938–19951. DOI: 10.1021/acs.iecr.0c03884

[13] Sakthivel, B., Josephine, D.S.R., Sethuraman, K., Dhakshinamoorthy, A. (2018). Oxidation of styrene using TiO2-graphene oxide composite as solid heterogeneous catalyst with hydroperoxide as oxidant. *Catal. Commun.*, 108, 41-45. DOI: 10.1016/j.catcom.2018.01.029

[14] Milovac, D., Weigand, I., Kovaˇci´c, M., Ivankovi´c, M., Ivankovi´c, H. (2018). Highly porous hydroxyapatite derived from cuttlefish bone as TiO2 catalyst support. *Proc. Appl. Ceramics*, 12(2), 136-142. DOI: 10.2298/PAC1802136M.

[15] Gawande, M.B., Bonifácio, V.D.B., Luque, R., Branco, P.S., Varma, R.S. (2013) Benign by design: catalyst-free in-water, on-water green chemical methodologies in organic synthesis. *Chem. Soc. Rev.*, 42, 5522-5551. DOI: 10.1039/C3CS60025D

[16] Ghuo, Z., Luo, B., Zhang, Q., Deng, W., Wang, Y., Yang, Y. (2014). Recent advances in heterogeneous selective oxidation catalysis for sustainable chemistry. *Chem. Soc. Rev.*, 43, 3480–3524. DOI: 10.1039/C3CS60282F

[17] Pan, Y., Shen, X., Yao, L., Bentalib, A., Peng, Z. (2018). Active site in heterogeneous catalytic reaction on metal and metal oxides: Theory and Practices. *Catalysts*, 8(10), 478. DOI: 10.3390/catal8100478

[18] Lin, P., Zhao, F., Ren, X., Lu, Y., Dong, X., Gao, L., Ma, T., Bao, J., Liu, A. (2024). Recent progress on Ti-based catalysts in the electrochemical synthesis of ammonia. *Nanoscale*, 16, 17300–17323. DOI: 10.1039/D4NR02852J

[19] Liu, S., Gao, J., Xu, W., Ji, Y., Zhu, T., Xu, G., Zhong, Z., Su, F. (2024). Transition metal-based catalysts for selective catalytic reduction of NO by CO: A state-of-the-art review. *Chem. Eng. J.*, 486, 150285. DOI: 10.1016/j.cej.2024.150285

[20] Lee, H., Wu, X., Sun, L. (2019) Copper-based homogeneous and heterogeneous catalysts for electrochemical water oxidation. *Nanoscale*, 12, 4187–4218. DOI: 10.1039/C9NR10437B

[21] Wen, C., Yin, A., Dai, W.L. (2014). Recent advances in silver-based heterogeneous catalysts for green chemistry processes. *Applied Catalysis B: Environmental*, 160-161, 730–741. DOI: 10.1016/j.apcatb.2014.06.016

[22] Chen, Y., Li, B., Xu, Y., Deng, L., Li, N., Peng, W. (2026). Quantitative description of structure-activity relationship for metal oxide catalysts in Fenton-Like reactions. *Chem. Eng. Sci.*, 321, 122865. DOI: 10.1016/j.ces.2025.122865

[23] Nilsson, A., Pettersson, L.G.M., Hammer, B., Bligaard, T., Nørskov, J.K., Christensen, C.K. (2005). The electronic structure effect in heterogeneous catalysis. *Catal. Lett.*, 100, 111–114. DOI: 10.1007/s10562-004-3434-9

[24] Chen, J., Zhang, Y., Zhang, Z., Hou, D., Bai, F., Han, Y., Zhang, C., Zhang, Y., Hu, J. (2023). Metal–support interactions for heterogeneous catalysis: mechanism, characterization techniques an applications. *J. Mater. Chem A.*, 11, 8540-8572. DOI: 10.1039/D2TA10036C

[25] Ito, S., Kon, Y., Nakashima, T., Hong, D., Ino, D., Sato, K. (2019) Titania-Catalyzed H2O2 Thermal Oxidation of styrenes to Aldehydes. *Mol.* 24, 1-9. DOI: 10.3390/molecules24142520

[26] Zhang, L.-X., Hua, Z.-L., Dong, X.-P., Li, L., Chen, H.-R., Shi, J.-L. (2007) Preparation of highly ordered Fe-SBA-15 by physical-vapor-infiltration and their application to liquid phase selective oxidation of styrene. *J. Mol. Catal. A: Chem.* 268, 155-162. DOI: 10.1016/j.molcata.2006.12.027

[27] Tong, J., Li, W., Wang, H., Hu, Y., Zhang, Z., Mahboo, A. (2016) Selective oxidation of styrene catalyzed by cerium-doped cobalt ferrite nanocrystals with greatly enhanced catalytic performance. *J. Catal.* 344, 474-481. DOI: 10.1016/j.jcat.2016.10.003

[28] Ghosh, S., Acharyya, S.S., Kumar, M., Bal, R. (2015). One-pot preparation of nanocrystalline Ag/WO3 catalyst for the selective oxidation of styrene. *Royal Soc. Chem. Adv.*. 5(47), 37610-37616. DOI: 10.1039/C5RA03803K

[29] Zhang, Y., Wang, H., Li, S., Lu, B., Zhao, J., Cai, Q. (2021). Catalytic oxidation of styrene and its reaction mechanism consideration over bimetal modified phosphotungstates. *Mol. Catal.* 515, 111940. DOI: 10.1016/j.mcat.2021.111940

[30] Zhang, D.-H., Li, H.-B., Li, G.-D., Chen, J.-S. (2009). Magnetically recyclable Ag-ferrite catalysts: general synthesis and support effects in the epoxidation of styrene. *Dalton Trans.*. 47, 10527-10533. DOI: 10.1039/b915232f

[31] Zou, H., Xiao, G., Chen, K., Peng, X. (2018). Noble metal free V2O5/g-C3N4 composite for selective oxidation of olefins using hydrogen peroxide as oxidant. *Dalton Trans.* 10, 1039-1047. DOI: 10.1039/C8DT02765J

[32] Wang, H., Qian, W., Chen, J., Wu, Y., Xu, X., Wang, J., Kong, Y. (2014). Spherical V-MCM-48: the synthesis, characterization and catalytic performance in styrene oxidation. *Royal Soc. Chem. Adv.* 4, 50832–50839. DOI: 10.1039/c4ra08333d

[33] Wan, Y., Liang, Q., Li, Z., Xu, S., Hu, X., Liu, Q., Lu, D. (2015). Significant improvement of styrene oxidation over zincphthalocyanine supported on multi-walled carbon nanotubes. *J. Mol. Catal. A: Chem.* 402, 29-36. DOI: 10.1016/j.molcata.2015.03.010

[34] Ramanathan, R., Sugunan, S. (2007). Styrene oxidation by H2O2 using Ni–Gd ferrites prepared by co-precipitation method. *Catal. Commun.* 8, 1521–1526. DOI: 10.1016/j.catcom.2006.12.021

[35] Tanglumlert, W., Imae, T., White, T. J., Wongkasemjit, S. (2009). Styrene oxidation with H2O2 over Fe- and Ti-SBA-1 mesoporous silica. *Catal. Commun.* 10, 1070-1073. DOI: 10.1016/j.catcom.2009.01.002

[36] Thao, N.T., Trung, H.H. (2014). Selective oxidation of styrene over Mg–Co–Al hydrotalcite like-catalysts using air as oxidant *Catal. Commun.* 45, 153-157. DOI: 10.1016/j.catcom.2013.11.004

[37] Cai, X., Wang, H., Zhang, Q., Tong, J. (2014). Selective oxidation of styrene efficiently catalyzed by spinel Mg–Cu ferrite complex oxides in water. *J. Sol-Gel Sci. Technol.*, 69, 33-39. DOI: 10.1007/s10971-013-3181-8

[38] Jiang, T., Gao, G., Yang, C., Mao, Y., Fang, M., Zhao, Q. (2020). Catalytic Activity of Ag-Co-MCM-41 for Liquid-Phase Selective Oxidation of Styrene to Benzaldehyde. *J. Nanosci. Nanotechnol.* 20, 1670–1677. DOI: 10.1166/jnn.2020.17137

[39] Sun, W., Hu, J. (2016). Oxidation of styrene to benzaldehyde with hydrogen peroxide in the presence of catalysts obtained by the immobilization of H3PW12O40 on SBA-15 mesoporous material. *React. Kin. Mechan. Catal.*, 119(1), 305-318. DOI: 10.1007/s11144-016-1024-7

[40] Wirawan, T., Nurhadi, M., Rahmadani, A., Prananto, Y.P., Zhu, Z., Lai, S.Y., Nur, H. (2023). One Pot Synthesis of Calcium Sulfate Hemihydrate from Fishbone-derived Carbon(Article). *Bull. Chem. React. Eng. Catal.*, 18(3), 398-406. DOI: 10.9767/bcrec.19515

[41] Nguyen, T.T.V., Anh, N.V., Ho, T.G.T., Pham, T.T.P., Nguyen, P.H.D., Do, B.L., Huynh, H.K.P., Nguyen, T. (2022). Hydroxyapatite Derived from Salmon Bone As Green Ecoefficient Support for Ceria-Doped Nickel Catalyst for CO2 Methanation. *ACS Omega*, 7(41), 36623-36633. DOI: 10.1021/acsomega.2c04621

[42] Borciani, G., Fischetti, T., Ciapetti, G., Montesiss,a M., Baldini, N., Graziani, G. (2023). Marine biological waste as a source of hydroxyapatite for bone tissue engineering applications. *Ceram. Int.*, 49(2), 1572-1584. DOI: 10.1016/j.ceramint.2022.10.341

[43] Tran, N.D.T., Che, T.N.H., Nguyen, T.T.V., Do, B.L., Ho, T.G.T., Nguyen, P.A., Pham, T.T.P., Tri, N., Ha, H.K.P. (2023). Fishbone derived-hydroxyapatite supported Ni-Zr nanocatalyst for CO2 methanation: Synergistic effects of support and zirconia. *Arab. J. Chem.*, 16(2), 105307. DOI: 10.1016/j.arabjc.2023.105307

[44] Sulaiman, S., Jamaludin, N.F,A., Kabbashi, N.A. (2019). Development of CaO/PVA Catalyst from Fish Bone for Biodiesel Production. *Bull. Chem. React. Eng. Catal.*, 14(1), 153-157. DOI: 10.9767/bcrec.14.1.3327.153-157

[45] Kusumawardani, R., Nurhadi, M., Wirawan, T., Prasetyo, A., Agusti, N.N., Lai, S.Y., Nur, H. (2022). Kinetic Study of Styrene Oxidation over Titania Catalyst Supported on Sulfonated Fish Bone-derived Carbon. *Bull. Chem. React. Eng. Catal.* 17(1), 194-204. DOI: 10.9767/bcrec.17.1.13133.194-204

[46] Liu, C., Zhao, Q., Wang, Y., Shi, P., Jiang, M. (2016). Surface modification of calcium sulfate whisker prepared from flue gas desulfurization gypsum. *Appl. Surface Sci.*, 360, 263-269. DOI: 10.1016/j.apsusc.2015.11.032

[47] Feng, X., Zhang, Y., Wang, G., Miao, M., Shi, L. (2015). Dual-surface modification of calcium sulfate whisker with sodium hexametaphosphate/silica and use as new water-resistant reinforcing fillers in papermaking. *Powder Technol.*, 271, 1-6. DOI: 10.1016/j.powtec.2014.11.015

[48] Dang, L., Nai, X., Zhu, D., Jing, Y., Liu, X., Dong, Y., Li, W. (2014). Study on the mechanism of surface modification of magnesium oxysulfate whisker. *Appl. Surface Sci.* 317, 325-331. DOI: 10.1016/j.apsusc.2014.07.205

[49] Duprey, E., Beaunier, P., Springuel-Huet, M.A., Bozon-Verduraz, F., Fraissard, J., Manoli, J.M, Brégeault, J.M. (1997). Characterization of Catalysts Based on Titanium Silicalite, TS-1, by Physicochemical Techniques. *J. Catal.*, 165(1), 22-32. DOI: 10.1006/jcat.1997.1462

[50] Liu, C., Huang, J., Sun, D., Zhou, Y., Jing, X., Du, M., Wang, H., Li, Q. (2013). Anatase type extra-framework titanium in TS-1: A vital factor influencing the catalytic activity toward styrene epoxidation. *Appl. Catal. A: Gen.*, 459, 1-7. DOI: 10.1016/j.apcata.2013.03.013

[51] Nur, H. (2006). Modification of titanium surface species of titania by attachment of silica nanoparticles. *Mater. Sci. Eng. B.* 133, 49-54. DOI: 10.1016/j.mseb.2006.05.003

[52] Nurhadi, M., Efendi, J., Lee, S.L., Mahlia, T.M.I., Chandren, S., Ho, C.S., Nur, H. (2015). Utilization of low rank coal as oxidation catalyst by controllable removal of its carbonaceous component. *J. Taiwan Inst. Chem. Eng.* 46(0), 183-190. DOI: 10.1016/j.jtice.2014.09.012

[53] Nurhadi, M., Kusumawardani, R., Wirawan, T., Lai, S.Y, Nur, H. (2023). Synergistic Ti-Fe Oxides on Fishbone-Derived Carbon Sulfonate: Enhanced Styrene Oxidation Catalysis. *Ind. J. Chem.* 23(6), 1514-1524. DOI: 10.22146/ijc.80667

[54] Lubis, S., Yuliati, L., Lee, S.L., Sumpono, I., Nur, H. (2012) Improvement of catalytic activity in styrene oxidation of carbon-coated titania by formation of porous carbon layer. *Chem. Eng. J.* 209, 468-493. DOI; 10.1016/j.cej.2012.08.041

[55] Indira, V., Halligudi, S.B., Gopinathan, S., Gopinathan, C. (2001). Kinetics and Mechanism of Styrene Oxidation Using Transition Metal Substituted Dodecatungstophosphate. *React. Kinet. Catal. Lett.* 73(1), 99-107. DOI: 10.1023/A:1013985123468.